HHS Public Access

Author manuscript

Radiat Res. Author manuscript; available in PMC 2016 September 16.

Published in final edited form as:

Radiat Res. 2015 December ; 184(6): 639–649. doi:10.1667/RR14178.1.

Whole lung irradiation results in pulmonary macrophage alterations that are subpopulation and strain specific

Angela M. Groves[a,*], **Carl J. Johnston**[a,b], **Ravi S. Misra**[a], **Jacqueline P. Williams**[b], and **Jacob N. Finkelstein**[a,b]

[a]Department of Pediatrics M&D Neonatology, University of Rochester Medical Center, Rochester, New York

[b]Department of Environmental Medicine, University of Rochester Medical Center, Rochester, New York

Abstract

Exposure of the lung to radiation produces injury and inflammatory responses that result in microenvironmental alterations that can promote the manifestation of pneumonitis and/or pulmonary fibrosis at later times. Following some other toxic insults, it has been shown that macrophages become phenotypically polarized in response to microenvironmental signals, orchestrating the downstream inflammatory responses; however, their contribution to the development of the late consequences of pulmonary radiation exposure is unclear. To address this issue, we exposed fibrosis-prone C57BL/6J or pneumonitis-prone C3H/HeJ mice to 0 or 12.5 Gy whole lung irradiation and lung digests were collected between 3 and 26 weeks following exposure. CD45+ leukocytes were isolated and characterized by flow cytometry; alveolar, interstitial, and infiltrating macrophages also were identified. Expression of Ly6C, expressed by pro-inflammatory monocytes and macrophages, and mannose receptor (CD206), a marker of alternative activation, were assessed in each subpopulation.

While the total number of pulmonary macrophages was depleted at 3 week following lung irradiation relative to age-matched controls in both C57 and C3H mice, identification of discrete subpopulations showed that this loss in cell number occurred in the alveolar, but not the interstitial or infiltrating, subsets. In the alveolar macrophages of both C57 and C3H mice, this correlated with a loss in the proportion of cells that expressed CD206 and F4/80. In contrast, in interstitial and infiltrating macrophages, the proportion of cells expressing these markers were increased at several time points following irradiation, with this response generally being more pronounced in C3H mice. Radiation exposure also was associated with elevations in the proportion of alveolar and interstitial macrophage subpopulations expressing Ly6C and F4/80, with this response occurring at earlier time points in C57 mice. Although the radiation dose used in this study was not isoeffective for the inflammatory response in the two strains, nonetheless the differences observed in the responses of these discrete macrophage populations between the fibrosis-prone versus pneumonitis-prone mice suggest a possible role for these cells in the development of long-term consequences of pulmonary irradiation.

Corresponding author: Angela M. Groves, Ph.D., Department of Pediatrics M&D Neonatology, University of Rochester Medical Center, 601 Elmwood Ave., Box 850, Rochester, NY 14642, angela_groves@urmc.rochester.edu.

*Scholar in Training

INTRODUCTION

Exposure of the lung to ionizing radiation results in cytotoxicity, seen particularly within the pulmonary parenchyma within hours to days post-exposure (1, 2). As a result of this injury, a depletion of resident immune cell populations is observed, although an acute inflammatory reaction also arises, in which pro-inflammatory cytokines and chemokines are released, attracting immune cells to the site(s) of injury (3). Following this immediate wound healing response, the normal architecture of the lung appears gradually to be restored, however it is apparent that a dysregulation of the pulmonary microenvironment persists. Within several months, or even years in humans, the failure to fully repair and resolve lung injury results in a dose-dependent migration of inflammatory and stromal cell progenitor populations into the lung, leading to the development of the clinically-recognized acute and late complications of pneumonitis and pulmonary fibrosis, respectively (2, 4). While collagen accumulation, fibroblast proliferation and tissue remodeling characterize the late fibrotic phase, the onset and progression of radiation pneumonitis is associated with an accumulation of monocytic inflammatory infiltrates. Indeed, investigators have shown that pulmonary macrophages undergo alterations in gene expression and cytokine and inflammatory mediator production following exposure to ionizing radiation, and have, therefore, been implicated in the development of the long-term radiation outcomes (5–8).

Multiple subpopulations of macrophages exist in the lung, residing in both the alveolar and interstitial compartments (9, 10). In addition, following injury or infection, infiltrating monocytes migrate into the lung from the circulation where they differentiate into macrophages, not only to contribute to renewing and maintaining resident subpopulations, but also to aid in inflammation and repair (11–13). As part of their pleiotropic nature, macrophages are plastic cells that can be differentially activated in a phenotypic-dependent manner to regulate inflammatory processes (14). For example, classically activated macrophages stimulate inflammatory responses, while alternatively activated macrophages promote repair and the resolution of inflammation (14–17). However, when macrophage polarization becomes dysregulated, inflammation can be enhanced or chronically prolonged in a pathological manner (18). Indeed, a disruption in the balance of these distinct populations is thought to contribute to the pathogenesis of many disorders, but the manner in which radiation may uniquely affect pulmonary macrophage subpopulations is not understood and is the focus of these studies.

The utilization of fibrosis-prone C57BL/6J (C57) and -resistant C3H/HeJ (C3H) mice is a strategy that has been used by multiple investigators to understand the potential differential processes that contribute to the early versus long-term consequences of lung exposure to radiation (3, 19–24). Whole thorax exposure to radiation causes an early, mild inflammation or pneumonitis, followed by an increase in collagen production and the development of fibrotic foci in C57 mice, whereas in C3H mice, pneumonitis is the predominant morbid effect and fibrogenesis does not occur (20, 24). Since we hypothesized that the macrophage subsets that repopulate the lung following radiation-induced depletion would be responding to an altered microenvironmental phenotype from those of unirradiated mice, we believed that these populations would differ between the strains since they demonstrate a different

pulmonary outcome. Therefore, to test this hypothesis, C3H and C57 mice were exposed to 12.5 Gy whole lung radiation and the response of their macrophage populations was characterized over the following 26 wk, at various time points across the course of pathogenesis. Specifically, radiation-induced effects on macrophage subpopulation depletion, recovery and phenotype were assessed.

MATERIALS AND METHODS

Animals

C57BL/6J and C3H/HeJ mice (female, 6–8 wk of age) obtained from Jackson Laboratory (Bar Harbor, ME) were housed 5 animals per cage under pathogen-free conditions and acclimated for one week prior to experimentation. Animals were fed standard laboratory diet and water *ad libitum*. The University Committee on Animal Resources approved all animal protocols.

Irradiation

Animals, restrained in plastic jigs, received a 12.5 Gy lung only exposure to a ^{137}Cs γ-ray source operating at a dose rate of approximately 1.8 Gy/min. Age-matched 0 Gy control mice were sham irradiated with identical handling.

Sample Collection

Mice were euthanized at 3, 8, 16, and 26 wk following irradiation. These time points were chosen since they represent the immediate (3 wk), pre- and post-pneumonitis (8, 16 wks) and pre-fibrosis response phases seen during progression to radiation-induced lung effects. Lung digests were obtained via instillation with 1.8 units/ml dispase (Gibco Life Technologies, Grand Island, NY) in DMEM (Gibco Life Technologies) and incubated at room temperature for 45 min. Lungs were then disrupted by mincing and the cell solution filtered through 100, 40, and 25 μm cell strainers (Fisher Scientific, Waltham, MA) using DMEM plus 0.01% DNAse-1 (Sigma, St Louis, MO) as a wash buffer, and then transferred to DMEM plus 10% FBS (BD Biosciences, San Jose, CA). Alternatively, the left lobe of the lung was inflation fixed in 10% zinc buffered formalin (Anatech, Battle Creek, MI) and paraffin embedded. Tissue sections (6 μm) were prepared and stained with Hematoxylin and Eosin or Gomori trichrome and examined by light microscopy. Images were acquired on an Olympus BX51 microscope (Olympus America, Center Valley, PA).

Magnetic Cell Sorting and Flow Cytometry

Lung digest cells were enriched for CD45+ myeloid cells by incubating with a biotin anti-CD45 antibody (BD Pharmingen, San Jose, CA) followed by binding to BD IMag Strepavidin Particles Plus (BD Biosciences), then placed on a Magna grIP magnet (Millipore, Billerica, MA). Unbound CD45− cells were then removed and CD45+ cells that were retained on the magnet were resuspended in DMEM plus 10% FBS. CD45+ cells were then counted using a hemocytometer and 1×10^6 cells were stained for flow cytometric analysis. Cells were transferred to staining buffer (PBS plus 10% FBS). Non-specific antibody binding was blocked using anti-mouse CD16/CD32 Fc block (BD Pharmingen) at 1:500 in staining buffer for 10 min on ice. Surface staining was then performed for 30 min at

4°C using PerCP-Cy5.5 Rat anti-mouse CD-11b (BD Pharmingen), Alexa Fluor 647 anti-mouse Ly6G, Brilliant Violet-605 anti-mouse CD206, Brilliant Violet 711 anti-mouse Ly6C, PE anti-mouse CD45 (Biolegend, San Diego, CA), eFluor 450 anti-mouse CD11c, and PE/Cy7 anti-mouse F4/80 (eBioscience, San Diego, CA). Following surface staining, cells were washed and stained with LIVE/DEAD fixable aqua dead cell stain kit (Life Technologies) in PBS for 15 min at 4°C. Cells were then washed, resuspended in 2.5% phosphate buffered formalin (Fisher Scientific) and run on an 18-paramater LSRII flow cytometer (BD Biosciences). For single color positive controls, Simply Cellular anti-mouse compensation standard (Bangs Laboratories, Fishers, IN) was incubated with 1 μl of each detection antibody. Data were analyzed using FlowJo (FlowJo, Ashland, OR).

Statistical Analysis

Data are expressed as mean ± SEM and were analyzed by two-way ANOVA, followed by Tukey's multiple comparisons test. Differences were considered significant at $P < 0.05$.

RESULTS

Characterization of Pulmonary Macrophage Subpopulations

To investigate the possibility that macrophage populations in the lung contribute to the long term consequences of radiation exposure, resident and infiltrating pulmonary macrophage subsets were investigated at time points spanning radiation-induced depletion and repopulation, through the development of long term outcomes. To confirm a differential pulmonary injury response to whole lung radiation between the two strains, histological sections were examined at the chosen time points for the presence of inflammatory cells and/or collagen accumulation. In both C57 and C3H mice, inflammation was observed at 8 wks post-radiation, with increased numbers of inflammatory cell infiltrates still being observed in the lung at 16 wk, defining the characteristic pneumonitic response period (Suppl. Fig. 1). This response was slightly more robust in the C3H mice, although no mortality was observed. Additionally, fibrotic foci were observed in C57, but not C3H mice, at 26 wk post radiation (Suppl. Fig. 2).

Since multiple distinct macrophage subpopulations exist in the lung, the individual responses of these subpopulations to radiation-induced lung injury were evaluated next. To accomplish this, we characterized pulmonary macrophage populations using flow cytometry. Dispase digested and CD45+ enriched lung cells were stained with macrophage- and phenotype-specific cell surface markers and analyzed. Viable CD45+, Ly6G− cells were first gated to distinguish myeloid cells and exclude neutrophils from further analysis of macrophage subpopulations (Fig. 1A). Individual macrophage subpopulations were next distinguished by analysis of expression of the cell surface markers CD11b and CD11c, which have been shown to be expressed on pulmonary macrophages to varying degrees depending on their anatomical location in the lung. Alveolar macrophages (AMs) (CD11b low, CD11c+), interstitial macrophages (IMs) (CD11b+, CD11c int) and infiltrating macrophages (CD11b+, CD11c−) (25–27) were each gated and separately analyzed for expression of the macrophage phenotype markers, F4/80, CD206, and Ly6C (Fig. 1B). A representative sample of this strategy is shown in Figure 1.

Regardless of strain and radiation exposure, AMs were found to be predominantly F4/80+ and CD206+, with few being Ly6C+, whereas a smaller proportion of IMs and infiltrating macrophage expressed CD206 and F4/80 (Fig. 1B). Similarly to AMs, the majority of IMs did not express Ly6C, while infiltrating macrophages consisted of both Ly6C+ and Ly6C− cells. Within the infiltrating population, a portion was found to be F4/80+ and expressed Ly6C with greater intensity than the F4/80− population. Since monocytes express F4/80 with varying levels of Ly6C, and are CD11b+ and CD11c−, it is likely that the F4/80+ population of the infiltrating macrophage subset is newly trafficked monocytes (28, 29).

Since alveolar macrophages are highly autofluorescent cells (30), the autofluorescent properties of the CD45+, Ly6G− population were assessed as a means of confirming AM identity (Fig. 1A). Distinct populations of autofluorescent positive and negative cells could be distinguished in the CD45+, Ly6G− population. The autofluorescent positive cells were found to be AMs as they were CD11b intermediate, CD11c+, F4/80+, and CD206+. In contrast, the autofluorescent negative cells varied in their expression of the cell surface markers, and were comprised of multiple macrophage subtypes that included the IM and infiltrating populations. Cell surface marker expression was also analyzed for the CD45+, Ly6G+ granulocyte population, which was found to be comprised of CD11b+ cells, the majority of which also expressed Ly6C.

Radiation Exposure Results in Pulmonary Macrophage Depletion and Repopulation

As demonstrated in Figure 1C, changes in the numbers of each subpopulation were examined over a time course covering the immediate, acute and late phases of injury (31). Within each subpopulation, alterations in the proportion of the cells expressing classical and alternative macrophage activation markers were characterized. To identify and characterize AMs, viable CD45+, Ly6G−, autofluorescent+ cells were gated on, then the CD11b int, CD11c+ population was selected for further analysis (Fig. 2A).

AMs made up the largest portion of the CD45+ cells recovered from the lung digests in both C3H and C57 mice. In unirradiated mice, at least 70% of AMs were positive for both CD206 and F4/80 (Fig. 2C), with fewer than 10% being F4/80 and Ly6C+ (Fig. 2D). It was noted that the baseline numbers of AMs were significantly higher in the C3H versus C57 mice at the 3 wk and 8 wk time points, possibly reflecting a more proinflammatory phenotype, although both strains demonstrated an age-related decline in AM numbers across the 6 month time course. Following irradiation, and consistent with previous studies (32), a decrease in AM cell number was observed at the 3 wk time point in both C3H and C57 mice, followed by a return to levels similar to those observed in sham irradiated mice. This occurred by 8 wk post-exposure in C57 mice, although in irradiated C3H mice a small, but significant, difference was observed until 16 wk following irradiation (Fig. 2B). Furthermore, as hypothesized, the phenotype of AMs repopulating the irradiated lungs was differentially altered when compared to AMs isolated from the age-matched control mice. As such, a decrease in the percentage of CD206+, F4/80+ AMs population was noted at the 3 wk time point in the C3H mice, followed by a return to control values, although an additional decline was seen at 26 wk post-radiation (Fig. 2C). This response was more exaggerated in the C57 mice when compared to C3H mice at 3 wk post-radiation, with

significant decreases in this population also present at both 8 and 26 wk post-radiation. In contrast, the percentage of Ly6C+, F4/80+ AMs were increased following irradiation. This was noted at the 8 and 16 wk time points in the C3H mice, and at the 3 and 16 wk time points in the C57 mice (Fig. 2D). This response occurred earlier, by 3 wk following exposure, in C57 mice.

IMs were identified by gating on viable CD45+, Ly6G−, autofluorescent− cells, and then gating on the CD11b+, CD11c+ population (Fig. 3A). In contrast to the observed AM response, the numbers of IMs were increased at 3 wk in C3H mice and at 8 wk following exposure in both strains of mice (Fig. 3B); again, irradiation induced alterations in macrophage phenotype in a strain-specific manner. An increase in the percentage of CD206+, F4/80+ cells in the IM population was observed at 3 wk and 8 wk post-radiation in C3H mice (Fig. 3C), accompanied at 8 wk by an increase in the Ly6C+, F4/80+ cells (Fig. 3D). In contrast, in C57 mice, a significant increase in percentage of Ly6C+, F4/80+ cells was observed only at 3 wk post exposure, a response not present in C3H mice. At all other time points, there was a trend towards a decrease in the percentage of both CD206+, F4/80+ and Ly6C+, F4/80+ cells (Figs. 3C and 3D), achieving a level of significance at 8 wk and 16 wk in the CD206+, F4/80+ cells. Interestingly, the overall percentage of these cells was also higher in the C57 control animals relative to the C3Hs (Fig. 3C).

CD11b high infiltrating cells were identified as CD45+, Ly6G−, autofluorescent−, CD11b high and CD11c− (Fig. 4A). A radiation-induced increase in the number of CD11b high infiltrating cells was observed in C57 mice, but not C3H mice (Fig. 4B). This response persisted for at least 8 wk following exposure before returning to values similar to those of age-matched control mice. While no significant changes were noted in overall CD11b high infiltrating cell number in C3H mice, the percentage of CD206+, F4/80+ cells in this population was increased following irradiation at the 3 wk through the 16 wk time points (Fig. 4C). The proportion of these cells were also increased in irradiated C57 mice, but the extent to which this occurred was not as large and was only observed through 8 wk post exposure. Furthermore, changes in the percentage of CD206+, F4/80+ cells in the CD11b high infiltrating subpopulation in irradiated C3H mice were inversely related to the percentage of Ly6C+ cells in this (Fig. 4D), whereas no loss in the proportion of Ly6C+, F4/80+ cells was observed in C57 mice. Instead, a significant increase in the percentage cells expressing these markers was observed at the 16 wk time point following exposure, which was maintained through 26 wk.

CD11b low infiltrating cells were identified as CD45+, Ly6G−, autofluorescent−, CD11b low, and CD11c− (Fig. 5A). A significant decrease in the number of CD11b low infiltrating cells was observed at 3 wk post-irradiation in C3H mice, before returning to values similar to those of age-matched controls (Fig. 5B). In C57 mice, a significant increase was noted in the number of cells in this population at 8 wk post-irradiation. Interestingly, in C3H mice, the percentage of CD206+, F4/80+ cells in this subpopulation increased relative to controls by 3 wk following exposure (Fig. 5C), whereas the percentage of Ly6C+ cells showed a sharp decrease at the 8 wk and 16 wk post exposure time points (Fig. 5D). The percentage of CD206+, F4/80+ cells was also increased in C57 mice at the 3 wk time point (Fig. 5C),

however the proportion of Ly-6C+ cells were not significantly altered when compared with age-matched controls (Fig. 5D).

Lung granulocytes (PMNs) were identified by gating on CD45+ Ly6G+ cells (Fig. 6A). Differences in this cell population were observed between the control animals of the two strains, with C3Hs having a greater number of these cells than C57s at multiple time points. The irradiated cohort of C3H mice demonstrated a reduction in neutrophils at the later time points (Fig. 6B), and decreases in the percentage of PMNs expressing Ly6C could be observed at 3 wk and 8 wk post exposure in C3H mice but not C57 mice (Fig. 6C).

DISCUSSION

Radiation-induced lung injury occurs in distinct phases, with acute wound healing being followed by early inflammation. However, it is believed that these phases involve the propagation of a chronic dysregulation of the lung microenvironment, resulting in the gradual development of the acute and late consequences, radiation pneumonitis and pulmonary fibrosis, respectively (2, 4). Although these outcomes are well characterized, the mechanisms underlying their development remain unclear. Under normal wound healing conditions, the clearance of dead cells and the release of inflammatory mediators, such as reactive oxygen species, cytokines and chemokines, by injured pulmonary epithelial cells initiate an acute inflammatory/wound healing response in the lung that is essential to its early recovery. Subsequently, recruited and activated immune cells promote repair of damaged tissue in part by initiating profibrotic responses. For example, activated macrophages recruit fibroblasts to the site of injury and interact with collagen-producing myofibroblasts. Macrophages also secrete transforming growth factor-B, which stimulates the production of extracellular matrix proteins and regulates the turnover of the extracellular matrix through production of matrix metalloproteinases and tissue inhibitors of matrix metalloproteinases (33, 34). However, following radiation-induced lung injury, it appears that these canonical inflammatory and profibrotic processes fail to completely resolve. Thus dysregulation can progress to overt inflammation and also may be associated with excess production of extracellular matrix components and tissue remodeling, the manifestations of alveolitis and pulmonary fibrosis, respectively.

Immune dysregulation, observed as part of the progression of radiation-induced events, likely results from the altered microenvironment of the irradiated lung. Importantly, macrophages are highly plastic cells that are adept at responding to microenvironmental signals, becoming phenotypically polarized in order to orchestrate inflammatory responses (14, 35). As a result of their observed involvement in the pulmonary response to radiation, dysregulation of macrophage activation has been implicated in the pathogenic processes that result in radiation-related chronic inflammation and fibrosis (36–41). Since exposure of the lung to radiation is known to initially deplete pulmonary macrophages (31), we investigated whether those macrophages subsequently repopulating the lung are phenotypically different compared to those found in unirradiated mice. The lung contains a heterogeneous population of macrophages that have specialized functions based on their anatomical location, with AMs and IMs having different functional properties, playing distinct roles in the lung and differing in their responses to inflammation and injury (10, 25, 42, 43). For example, AMs

are a long-lived, self-renewing population with a turnover rate of 40% in 1 year and are efficient at removing microorganisms and particles from the lung (10, 44–46). In contrast, IMs function as antigen presenters and regulators of inflammation and fibrosis and are thought to be replaced by infiltrating monocytes that migrate into the lung from the circulation (11, 13, 25). We therefore investigated whether radiation injury may differentially affect either these specific populations or their response to a radiation altered microenvironment.

Distinguishing between the different macrophage subpopulations in the lung allows for an individual evaluation to be made of each subset and eliminates the possibility of erroneously interpreting the actions of multiple macrophage subpopulations as a single response. Consequently, our findings illustrate that these distinct populations do indeed differ in their response to radiation exposure. Following identification of AM, IM and infiltrating macrophage subsets, it was revealed that the loss of lung macrophages observed at 3 wk following radiation was apparent in the AM, but not the interstitial or infiltrating, populations in both C3H and C37 mice, which instead appeared to be above control values at this time point. However, only a cautious interpretation can be made of this observation since the periodicity of the sampling means that this finding may not reflect the response of the subpopulations from the time of irradiation. Indeed, it is possible that IMs, with a comparatively high turnover rate, may be an intermediate between infiltrating and alveolar populations (11) and, therefore, may recover more quickly than do the more slowly replicating AM population from the cell losses that occurred as a direct result of radiation-induced lung injury. Alternatively, although not significant contributors to resident macrophage populations during homeostasis, monocytes have been found to be capable of replacing interstitial and alveolar populations of macrophages in mice following lung inflammation (44, 46, 47) and it is therefore possible that, following radiation, infiltrating macrophages first replenished the depleted interstitial populations, which could in turn contribute to the later restoration of the alveolar population.

The differing sensitivities of C57 and C3H mice to developing pneumonitis and fibrosis following exposure to radiation have been exploited in attempts to uncover the mechanisms involved in these processes. Previous studies have observed pneumonitis occurring in both C3H and C57 mice following radiation exposure, with this response being sufficiently robust in C3H mice that it can lead to morbidity; however, the dose used in this study (12.5 Gy) did not reach this threshold. In contrast, the pneumonitic response in C57 mice is mild and, often, asymptomatic even at higher doses; nonetheless, these animals exhibit pathologic progression and will develop dose- and volume-dependent fibrotic lesions not seen in the C3H survivors (19, 23). These observations are supported by experiments from our lab demonstrating that TGF-beta expression, as well as collagen mRNA expression and production, increased in the lungs of C57, but not C3H, mice following exposure to 12.5 Gy radiation (20).

Since differing responses of pulmonary macrophages subsets to radiation could be dependent on their phenotype prior to exposure, macrophage expression of the phenotypic markers CD206 (mannose receptor), associated with alternative activation of macrophages and a means by which AMs repress inflammatory responses to maintain homeostasis in the

lung, and Ly6C, a marker associated with pro-inflammatory responses, were first determined in unirradiated mice (29, 48, 49). The finding that the majority of AMs expressed CD206, while less than 25% of IMs and less than half of infiltrating macrophages expressed this marker is in line with studies showing that mannose receptor is predominately expressed by alveolar macrophages since it is a carbohydrate-binding C-type lectin that functions to maintain a quiescent state in the lung by interacting with pathogens and suppressing proinflammatory responses (49, 50). In contrast the majority of infiltrating macrophages were Ly6C+, whereas less than 10% of AMs and IMs expressed this marker. Analysis of these markers also revealed significant baseline strain differences in pulmonary macrophage subsets. Differences were noted in numbers of AMs recovered from the lungs of unirradiated C3H and C57 mice at early time points and variance in phenotypic markers were also present. This suggests that inherent differences in the pulmonary macrophage subpopulations may affect the differential lung responses of these two strains to radiation and highlight that genetic factors are an important determinant of radiation outcomes. Further investigation of how genetic variation predicts the likelihood of developing pneumonitis and fibrosis will be important for assessing the individual susceptibility of humans to radiation-induced pathologies following treatment or unforeseen exposure.

With respect to early changes following radiation exposure, in both C3H and C57 mice, a reduction was observed in the proportion of CD206+, F4/80+ AMs by 3 wk that correlated with the depletion in AM cell numbers. This decline may not necessarily represent radiation-induced cell loss; although nearly all AMs expressed CD206 in the unirradiated mice, this receptor may not yet be present on newly differentiated AMs if its expression is dependent on microenvironmental cues from alveoli. Indeed, studies have shown that lung macrophages respond to microenvironmental conditions and develop phenotypic characteristics accordingly. This was illustrated when adoptively transferred bone marrow and peritoneal macrophages in the lungs of mice acquired the same expression of certain cell surface markers as AMs (27). Although subject to inter-animal variability and the frequency of sample collection, the proportion of AMs expressing Ly6C was generally increased through 16 wk post irradiation in C57 mice, and at the 8 wk and 16 wk time points in the C3H mice, in an inverse association with the decreased proportion of CD206+ cells. This may have been the result of a shift in the AM population towards a proinflammatory phenotype, induced by an imbalance in proinflammatory versus profibrotic signaling following radiation exposure. Another possibility is that Ly6C-expressing monocytes, as well as IMs, have begun to differentiate into AMs in an attempt to maintain this population.

Importantly, further analysis of lung macrophage subsets revealed that the radiation-induced alterations in macrophage phenotype were highly strain-dependent. For example, the loss of CD206-expressing AMs occurred to a greater extent and for a longer period of time in C57 mice than in C3H mice, persisting beyond the point where the numbers of AMs had returned to values similar to unirradiated mice. This occurred in association with a more rapid increase in the proportion of AMs expressing Ly6C, suggesting that AMs from C57 mice were not as successful in maintaining an alternatively activated phenotype as those from C3H mice and were, instead, more prone to proinflammatory phenotype shifts. However, IMs and infiltrating macrophages exhibited different responses to radiation than AMs. In C3H mice, for at least 16 wk following exposure radiation increased the proportion of

CD206+ IMs and infiltrating macrophages and decreased the proportion of Ly6C+ infiltrating macrophages. In contrast, a pronounced alternative activation response was not observed in macrophage subpopulations of C57 mice. Indeed, radiation resulted in decreased, not increased, CD206 responses in IMs of C57 mice, while in the infiltrating populations, CD206 increases occurred to a lesser extent and for a shorter duration than in C3H mice. Moreover, C57 mice did not experience losses in the proportion of Ly6C+ CD11b high and low infiltrating populations that occurred in C3H mice. Instead proinflammatory phenotype shifts were more pronounced in C57 mice. Increases in the proportion of Ly6C+ CD11b high infiltrating macrophages were observed by 16 wk post radiation in C57 mice, whereas in C3H mice, this effect occurred later, by 26 wk, and was preceded by a loss of Ly6C+ cells, a response not observed in C57 mice. In AMs and IMs of C57 mice, the increased proportion of Ly6C-expressing cells in these populations also occurred earlier than in C3H mice. This suggests that, during the observed time course, C3H mice responded to radiation-induced injury through induction of an alternatively activated phenotype in lung macrophages, while in C57 mice, proinflammatory phenotypic shifts in the lung macrophage populations occurred. Interestingly in C3H mice, a decreased proportion of proinflammatory Ly6C+ infiltrating cells were observed following irradiation at time points peripheral to peak pneumonitis responses. Since the Ly6C+ population likely represents immature and newly trafficked infiltrating monocytes/macrophages, the loss of this marker at these time points may be reflective of a maturation of the infiltrating population with an accompanying loss of Ly6C. The fact that this loss was found to be accompanied by an increase in CD206 expression, suggests that it is possible that differing microenvironmental signals in the lungs of irradiated C57 and C3H mice result in differing abilities to induce proinflammatory immune responses. Since peak pneumonitis responses occur between the 8 wk and 16 wk time points, the fact that the alternative activation phenotype was more pronounced in the C3H mice could be indicative of their greater sensitivity to developing pneumonitis. Interestingly strain differences between unirradiated C3H and C57 mice were observed to be lessened with age. The fact that phenotypic differences in macrophages of irradiated animals were also minimized at these times suggests that the presence of unidentified age-related factors impact on macrophage activation responses. It is therefore possible that the relative contributions of macrophages on long-term clinical outcomes may vary not only with the time course of pathogenesis, but also with respect to the age of the patient.

Neutrophil populations were also affected by radiation exposure. Not only were greater numbers of Ly6G+ cells generally recovered from the lungs of unirradiated C3H mice, the radiation-induced alterations in this population were also more apparent than in C57 mice. This suggests strain differences in neutrophil trafficking and phenotype may influence their response to radiation-induced injury. In the first 8 wk following irradiation, a loss of Ly6C-expressing PMNs occurred in C3H mice but not C57 mice, correlating with the alterations observed in the infiltrating macrophage subsets. This is in accord with previous work that has found that radiation increases expression of several chemokines, including the macrophage inflammatory proteins and monocyte chemotactic protein-1 in the lungs of C57 mice, but not C3H mice (3). Furthermore, a radiation-induced increase in the numbers of CD11b high and low infiltrating macrophages was observed in C57 mice only. The

recruitment of inflammatory monocytes may affect the phenotype of the resident macrophage population, either through differentiation or through release of mediators that regulate macrophage polarization. This is supported by a study demonstrating that depletion of Ly6C hi circulating monocytes reduced fibrosis in mice exposed to bleomycin, whereas their adoptive transfer exacerbated fibrosis (38). A link between recruitment of inflammatory monocytes to the lung and the development of fibrosis has been demonstrated. Accumulations of Ly6C hi monocytes were found to occur following alveolar epithelial type 2 cell injury, while inhibition of this process abrogated collagen deposition (51).

As previously observed, radiation-induced phenotypic alterations in these macrophage populations persisted throughout the time course of this study and, possibly, throughout the lifespan of the mice. This chronic dysregulation of macrophage phenotype points to a contribution by these subpopulations to the development of long-term pathology. What remains unclear is whether these immune responses drive pathogenesis or are a consequence of the altered microenvironment of the lung parenchyma. Further studies are needed to address this question and to determine how these different phenotypic responses contribute to the different long-term pathologies in C57 and C3H mice. Increasing our understanding of how macrophages contribute to the differential pulmonary pathogenic processes will benefit our ability to develop effective mitigators of radiation-induced pathologies. Importantly, being able to use phenotypic markers in order to identify the patient populations at risk of developing late morbidities following radiation therapy will allow clinicians to tailor treatment to individual patients and minimize their subsequent risk of developing late effects.

Supplementary Material

Refer to Web version on PubMed Central for supplementary material.

References

1. Ward JF. Some Biochemical Consequences of the Spatial-Distribution of Ionizing Radiation-Produced Free-Radicals. Radiat Res. 1981; 86:185–95. [PubMed: 7015409]
2. Williams JP, Brown SL, Georges GE, Hauer-Jensen M, Hill RP, Huser AK, et al. Animal models for medical countermeasures to radiation exposure. Radiat Res. 2010; 173:557–78. [PubMed: 20334528]
3. Johnston CJ, Wright TW, Rubin P, Finkelstein JN. Alterations in the expression of chemokine mRNA levels in fibrosis-resistant and -sensitive mice after thoracic irradiation. Exp Lung Res. 1998; 24:321–37. [PubMed: 9635254]
4. Trott KR, Herrmann T, Kasper M. Target cells in radiation pneumopathy. Int J Radiat Oncol Biol Phys. 2004; 58:463–9. [PubMed: 14751516]
5. Chiang CS, Liu WC, Jung SM, Chen FH, Wu CR, McBride WH, et al. Compartmental responses after thoracic irradiation of mice: strain differences. Int J Radiat Oncol Biol Phys. 2005; 62:862–71. [PubMed: 15936571]
6. Coates PJ, Rundle JK, Lorimore SA, Wright EG. Indirect macrophage responses to ionizing radiation: implications for genotype-dependent bystander signaling. Cancer Res. 2008; 68:450–6. [PubMed: 18199539]
7. Johnston CJ, Williams JP, Elder A, Hernady E, Finkelstein JN. Inflammatory cell recruitment following thoracic irradiation. Exp Lung Res. 2004; 30:369–82. [PubMed: 15204829]

8. Zhang H, Han G, Liu H, Chen J, Ji XM, Zhou FX, et al. The Development of Classically and Alternatively Activated Macrophages Has Different Effects on The Varied Stages of Radiation-induced Pulmonary Injury in Mice. J Radiat Res. 2011; 52:717–26. [PubMed: 22104268]
9. Aggarwal NR, King LS, D'Alessio FR. Diverse macrophage populations mediate acute lung inflammation and resolution. Am J Physiol Lung Cell Mol Physiol. 2014; 306:L709–25. [PubMed: 24508730]
10. Hussell T, Bell TJ. Alveolar macrophages: plasticity in a tissue-specific context. Nat Rev Immunol. 2014; 14:81–93. [PubMed: 24445666]
11. Landsman L, Jung S. Lung macrophages serve as obligatory intermediate between blood monocytes and alveolar macrophages. J Immunol. 2007; 179:3488–94. [PubMed: 17785782]
12. Maus UA, Waelsch K, Kuziel WA, Delbeck T, Mack M, Blackwell TS, et al. Monocytes are potent facilitators of alveolar neutrophil emigration during lung inflammation: role of the CCL2-CCR2 axis. J Immunol. 2003; 170:3273–8. [PubMed: 12626586]
13. Yona S, Jung S. Monocytes: subsets, origins, fates and functions. Curr Opin Hematol. 2010; 17:53–9. [PubMed: 19770654]
14. Mosser DM, Edwards JP. Exploring the full spectrum of macrophage activation. Nat Rev Immunol. 2008; 8:958–69. [PubMed: 19029990]
15. Gordon S. Alternative activation of macrophages. Nat Rev Immunol. 2003; 3:23–35. [PubMed: 12511873]
16. Martinez FO. Regulators of macrophage activation. Eur J Immunol. 2011; 41:1531–4. [PubMed: 21607943]
17. Murray PJ, Allen JE, Biswas SK, Fisher EA, Gilroy DW, Goerdt S, et al. Macrophage activation and polarization: nomenclature and experimental guidelines. Immunity. 2014; 41:14–20. [PubMed: 25035950]
18. Laskin DL, Sunil VR, Gardner CR, Laskin JD. Macrophages and tissue injury: agents of defense or destruction? Annu Rev Pharmacol Toxicol. 2011; 51:267–88. [PubMed: 20887196]
19. Franko AJ, Sharplin J, Ward WF, Hinz JM. The genetic basis of strain-dependent differences in the early phase of radiation injury in mouse lung. Radiat Res. 1991; 126:349–56. [PubMed: 1852022]
20. Johnston CJ, Piedboeuf B, Baggs R, Rubin P, Finkelstein JN. Differences in correlation of mRNA gene expression in mice sensitive and resistant to radiation-induced pulmonary fibrosis. Radiat Res. 1995; 142:197–203. [PubMed: 7724735]
21. Johnston CJ, Piedboeuf B, Rubin P, Williams JP, Baggs R, Finkelstein JN. Early and persistent alterations in the expression of interleukin-1α, interleukin-1β and tumor necrosis factor α mRNA levels in fibrosis-resistant and sensitive mice after thoracic irradiation. Rad Res. 1996; 145:762–7.
22. Paun A, Kunwar A, Haston CK. Acute adaptive immune response correlates with late radiation-induced pulmonary fibrosis in mice. Radiat Oncol. 2015; 10:45. [PubMed: 25889053]
23. Sharplin J, AJ. A quantitative histological study of strain-dependent differences in the effects of irradiation on mouse lung during the intermediate and late phases. Radiat Res. 1989; 119:15–31. [PubMed: 2756106]
24. Ward WF, Sharplin J, Franko AJ, Hinz JM. Radiation-induced pulmonary endothelial dysfunction and hydroxyproline accumulation in four strains of mice. Radiat Res. 1989; 120:113–20. [PubMed: 2552496]
25. Misharin AV, Morales-Nebreda L, Mutlu GM, Budinger GR, Perlman H. Flow cytometric analysis of macrophages and dendritic cell subsets in the mouse lung. Am J Respir Cell Mol Biol. 2013; 49:503–10. [PubMed: 23672262]
26. Zaynagetdinov R, Sherrill TP, Kendall PL, Segal BH, Weller KP, Tighe RM, et al. Identification of Myeloid Cell Subsets in Murine Lungs Using Flow Cytometry. Am J Respir Cell Mol Biol. 2013; 49:180–9. [PubMed: 23492192]
27. Guth AM, Janssen WJ, Bosio CM, Crouch EC, Henson PM, Dow SW. Lung environment determines unique phenotype of alveolar macrophages. Am J Physiol Lung Cell Mol Physiol. 2009; 296:L936–46. [PubMed: 19304907]
28. Ingersoll MA, Spanbroek R, Lottaz C, Gautier EL, Frankenberger M, Hoffmann R, et al. Comparison of gene expression profiles between human and mouse monocyte subsets. Blood. 2010; 115:e10–e9. [PubMed: 19965649]

29. Sunderkotter C, Nikolic T, Dillon MJ, Van Rooijen N, Stehling M, Drevets DA, et al. Subpopulations of mouse blood monocytes differ in maturation stage and inflammatory response. J Immunol. 2004; 172:4410–7. [PubMed: 15034056]
30. Viksman MY, Liu MC, Schleimer RP, Bochner BS. Application of a Flow Cytometric Method Using Autofluorescence and a Tandem Fluorescent Dye to Analyze Human Alveolar Macrophage Surface-Markers. J Immunol Methods. 1994; 172:17–24. [PubMed: 8207263]
31. Rubin P, Johnston CJ, Williams JP, McDonald S, Finkelstein JN. A perpetual cascade of cytokines postirradiation leads to pulmonary fibrosis. Int J Radiat Oncol Biol Phys. 1995; 33:99–109. [PubMed: 7642437]
32. Hong JH, Jung SM, Tsao TCY, Wu CJ, Lee CY, Chen FH, et al. Bronchoalveolar lavage and interstitial cells have different roles in radiation-induced lung injury. Int J Radiat Biol. 2003; 79:159–67. [PubMed: 12745880]
33. Broekelmann TJ, Limper AH, Colby TV, Mcdonald JA. Transforming Growth Factor-Beta-1 Is Present at Sites of Extracellular-Matrix Gene-Expression in Human Pulmonary Fibrosis. P Natl Acad Sci USA. 1991; 88:6642–6.
34. Craig VJ, Polverino F, Laucho-Contreras ME, Shi Y, Liu Y, Osorio JC, et al. Mononuclear phagocytes and airway epithelial cells: novel sources of matrix metalloproteinase-8 (MMP-8) in patients with idiopathic pulmonary fibrosis. PloS one. 2014; 9:e97485. [PubMed: 24828408]
35. Liu YC, Zou XB, Chai YF, Yao YM. Macrophage polarization in inflammatory diseases. Int J Biol Sci. 2014; 10:520–9. [PubMed: 24910531]
36. Barkauskas CE, Noble PW. Cellular Mechanisms of Tissue Fibrosis. 7. New insights into the cellular mechanisms of pulmonary fibrosis. American Journal of Physiology-Cell Physiology. 2014; 306:C987–C96. [PubMed: 24740535]
37. Duffield JS, Forbes SJ, Constandinou CM, Clay S, Partolina M, Vuthoori S, et al. Selective depletion of macrophages reveals distinct, opposing roles during liver injury and repair. TJ Clin Invest. 2005; 115:56–65.
38. Gibbons MA, MacKinnon AC, Ramachandran P, Dhaliwal K, Duffin R, Phythian-Adams AT, et al. Ly6Chi monocytes direct alternatively activated profibrotic macrophage regulation of lung fibrosis. Am J Respir Crit Care Med. 2011; 184:569–81. [PubMed: 21680953]
39. Lech M, Anders HJ. Macrophages and fibrosis: How resident and infiltrating mononuclear phagocytes orchestrate all phases of tissue injury and repair. Bba-Mol Basis Dis. 2013; 1832:989–97.
40. Wynn TA. Integrating mechanisms of pulmonary fibrosis. J Exp Med. 2011; 208:1339–50. [PubMed: 21727191]
41. Whitsett JA, Alenghat T. Respiratory epithelial cells orchestrate pulmonary innate immunity. Nat Immunol. 2015; 16:27–35. [PubMed: 25521682]
42. Barletta KE, Cagnina RE, Wallace KL, Ramos SI, Mehrad B, Linden J. Leukocyte compartments in the mouse lung: Distinguishing between marginated, interstitial, and alveolar cells in response to injury. J Immunol Methods. 2012; 375:100–10. [PubMed: 21996427]
43. Johnston LK, Rims CR, Gill SE, McGuire JK, Manicone AM. Pulmonary macrophage subpopulations in the induction and resolution of acute lung injury. Am J Respir Cell Mol Biol. 2012; 47:417–26. [PubMed: 22721830]
44. Hashimoto D, Chow A, Noizat C, Teo P, Beasley MB, Leboeuf M, et al. Tissue-resident macrophages self-maintain locally throughout adult life with minimal contribution from circulating monocytes. Immunity. 2013; 38:792–804. [PubMed: 23601688]
45. Janssen WJ, Barthel L, Muldrow A, Oberley-Deegan RE, Kearns MT, Jakubzick C, et al. Fas determines differential fates of resident and recruited macrophages during resolution of acute lung injury. Am J Respir Crit Care Med. 2011; 184:547–60. [PubMed: 21471090]
46. Maus UA, Janzen S, Wall G, Srivastava M, Blackwell TS, Christman JW, et al. Resident alveolar macrophages are replaced by recruited monocytes in response to endotoxin-induced lung inflammation. Am J Respir Cell Mol Biol. 2006; 35:227–35. [PubMed: 16543608]
47. Cai Y, Sugimoto C, Arainga M, Alvarez X, Didier ES, Kuroda MJ. In vivo characterization of alveolar and interstitial lung macrophages in rhesus macaques: implications for understanding lung disease in humans. J Immunol. 2014; 192:2821–9. [PubMed: 24534529]

48. Swirski FK, Libby P, Aikawa E, Alcaide P, Luscinskas FW, Weissleder R, et al. Ly-6Chi monocytes dominate hypercholesterolemia-associated monocytosis and give rise to macrophages in atheromata. J Clin Invest. 2007; 117:195–205. [PubMed: 17200719]

49. Zhang J, Tachado SD, Patel N, Zhu J, Imrich A, Manfruelli P, et al. Negative regulatory role of mannose receptors on human alveolar macrophage proinflammatory cytokine release in vitro. J Leukoc Biol. 2005; 78:665–74. [PubMed: 16000387]

50. Pechkovsky DV, Prasse A, Kollert F, Engel KM, Dentler J, Luttmann W, et al. Alternatively activated alveolar macrophages in pulmonary fibrosis-mediator production and intracellular signal transduction. Clin Immunol. 2010; 137:89–101. [PubMed: 20674506]

51. Osterholzer JJ, Olszewski MA, Murdock BJ, Chen G-H, Erb-Downward JR, Subbotina N, et al. Implicating exudate macrophages and Ly-6chigh monocytes in CCR2-dependent lung fibrosis following gene-targeted alveolar injury. J Immunol. 2013; 190:3447–57. [PubMed: 23467934]

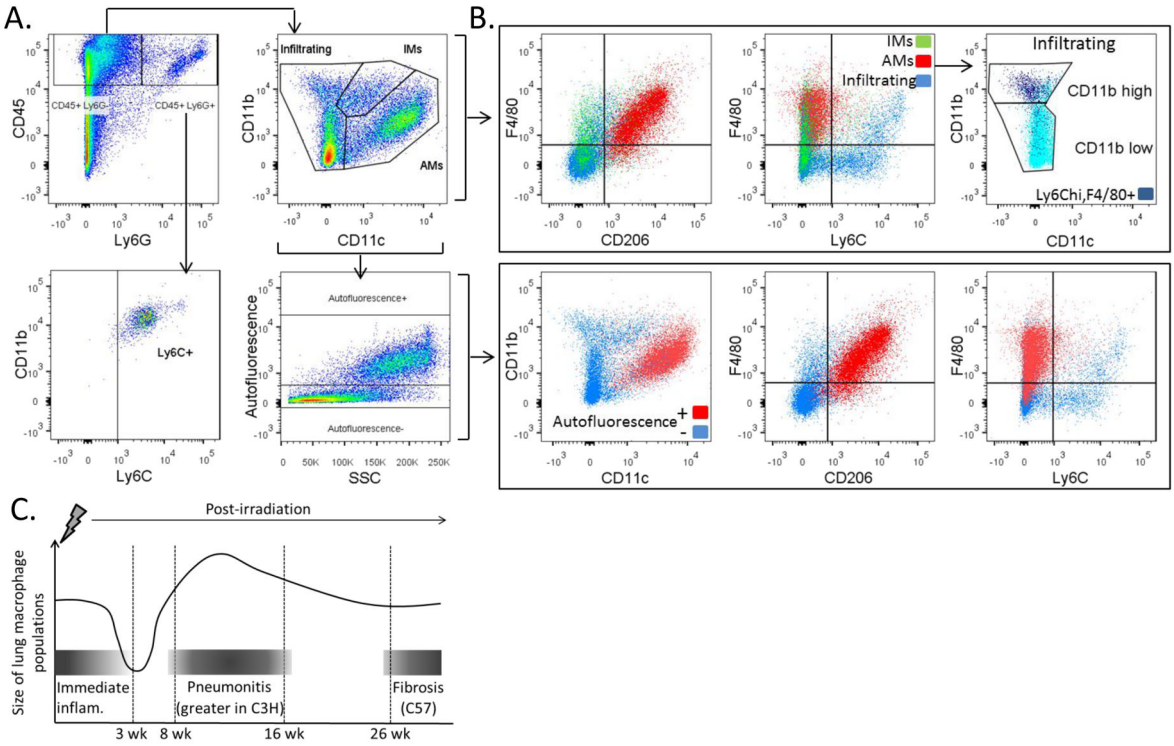

Figure 1.

Gating strategy and flow cytometric characterization of pulmonary macrophage populations. 1A: Lungs of C3H and C57 mice were dispase digested and enriched for CD45+ cells using MACS 3–26 wk following 12.5 Gy whole lung irradiation. Cells were stained with antibodies to CD45, Ly6G, CD11b, CD11c, F4/80, Ly6C and CD206 and analyzed by flow cytometry. A representative sample is shown. Pulmonary macrophage subpopulations were distinguished based on CD11b and CD11c expression. 1B: For each subpopulation, expression of F4/80, Ly6C and CD206 was characterized. Autofluorescence was also assessed in the CD45+, Ly6G− population and the expression of CD11b, CD11c, F4/80, Ly6C and CD206 determined in autofluorescent positive and negative subpopulations. Additionally, the CD45+, Ly6G+ population was analyzed for the expression of CD11b, F4/80 and Ly6C. 1C: Pattern of macrophage presence in lung following irradiation relative to known pathology and time points.

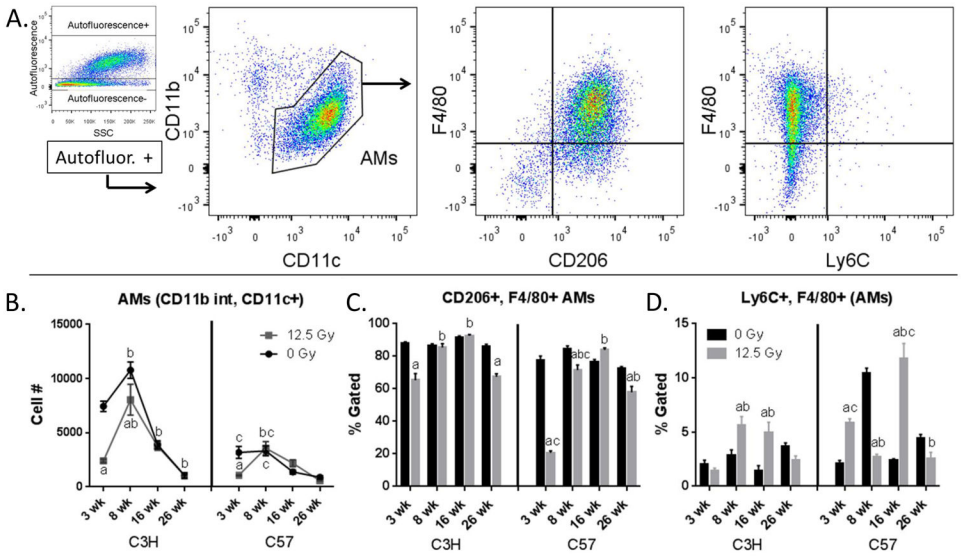

Figure 2.

Characterization of AMs. Lung cells from C3H and C57 mice, collected 3–26 wk following exposure of to 0 Gy or 12.5 Gy whole lung irradiation, were analyzed by flow cytometry. 2A: AMs were identified by first gating on autofluorescent+ cells in the CD45+, Ly6G− population and were identified as CD11b int and CD11c+. AMs were next analyzed for their expression of F4/80, Ly6C and CD206. One representative sample is shown. 2B: Radiation-induced alterations in AM cell number. 2C: Radiation-induced alterations in the proportion of CD206 and F4/80+ AMs. 2D: Radiation-induced alterations in the proportion of Ly6C+ and F4/80+ AMs. Each bar represents mean ± SEM (n = 3–4 mice/treatment group). [a]Significantly different from age-matched controls. [b]Significantly different from 3 wk time point (controls only). [c]Significantly different from C3H mice.

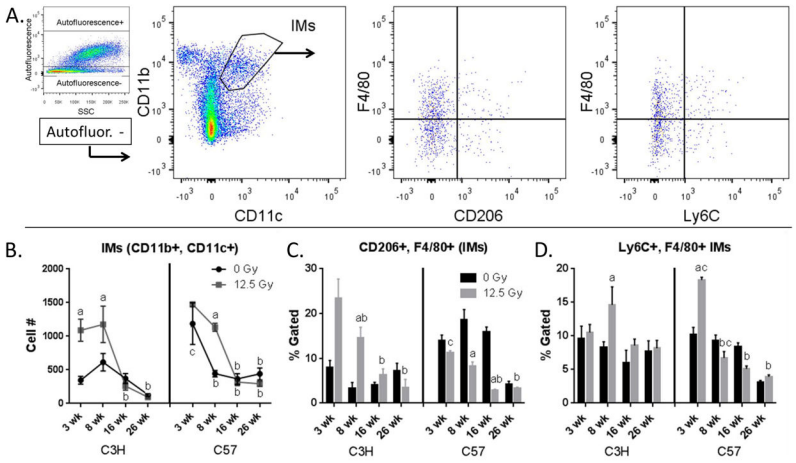

Figure 3.

Characterization of IMs. Lung cells from C3H and C57 mice, collected 3–26 wk following exposure of to 0 Gy or 12.5 Gy whole lung irradiation, were analyzed by flow cytometry. 3A: IMs were identified by first gating on autofluorescent− cells in the CD45+, Ly6G− population and were identified as CD11b+ and CD11c+. IMs were next analyzed for their expression of F4/80, Ly6C and CD206. One representative sample is shown. 3B: Radiation-induced alterations in IM cell number. 3C: Radiation-induced alterations in the proportion of CD206 and F4/80+ IMs. 3D: Radiation-induced alterations in the proportion of Ly6C and F4/80+ IMs. Each bar represents mean ± SEM (n = 3–4 mice/treatment group). [a]Significantly different from age-matched controls. [b]Significantly different from 3 wk time point (controls only). [c]Significantly different from C3H mice.

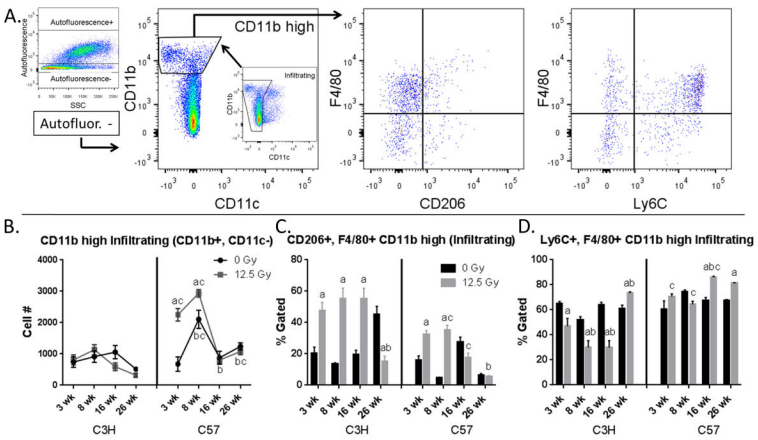

Figure 4.

Characterization of CD11b high infiltrating cells. Lung cells from C3H and C57 mice, collected 3–26 wk following exposure of to 0 Gy or 12.5 Gy whole lung irradiation, were analyzed by flow cytometry. 4A: CD11b high infiltrating cells were identified by first gating on autofluorescent− cells in the CD45+, Ly6G− population and were identified as CD11b+ and CD11c−. CD11b high infiltrating cells were next analyzed for their expression of F4/80, Ly6C and CD206. One representative sample is shown. 4B: Radiation-induced alterations in CD11b high infiltrating cell number. 4C: Radiation-induced alterations in the proportion of CD206 and F4/80+ CD11b high infiltrating cells. 4D: Radiation-induced alterations in the proportion of Ly6C and F4/80+ CD11b high infiltrating cells. Each bar represents mean ± SEM (n = 3–4 mice/treatment group). [a]Significantly different from age-matched controls. [b]Significantly different from 3 wk time point (controls only). [c]Significantly different from C3H mice.

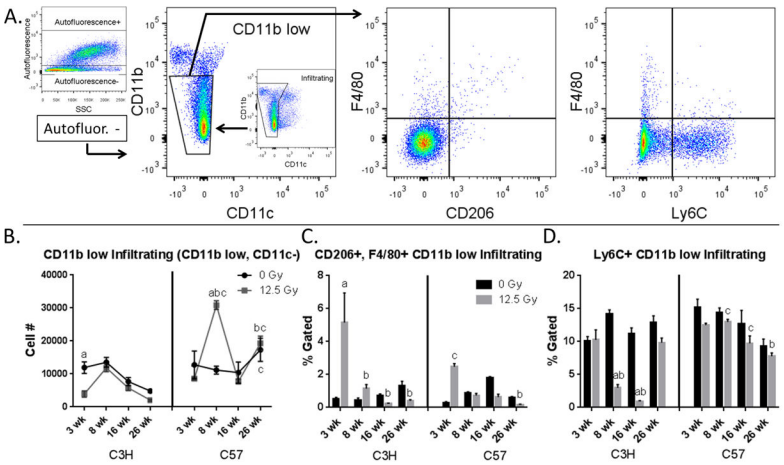

Figure 5.

Characterization of CD11b low infiltrating cells. Lung cells from C3H and C57 mice, collected 3–26 wk following exposure of to 0 Gy or 12.5 Gy whole lung irradiation, were analyzed by flow cytometry. 5A: CD11b low infiltrating cells were identified by first gating on autofluorescent− cells in the CD45+, Ly6G− population and were identified as CD11b int and CD11c−. CD11b low infiltrating cells were next analyzed for their expression of F4/80, Ly6C and CD206. One representative sample is shown. 5B: Radiation-induced alterations in CD11b low infiltrating cell number. 5C: Radiation-induced alterations in the proportion of CD206 and F4/80+ CD11b low infiltrating cells. 5D: Radiation-induced alterations in the proportion of Ly6C and F4/80+ CD11b low infiltrating cells. Each bar represents mean ± SEM (n = 3–4 mice/treatment group). [a]Significantly different from age-matched controls. [b]Significantly different from 3 wk time point (controls only). [c]Significantly different from C3H mice.

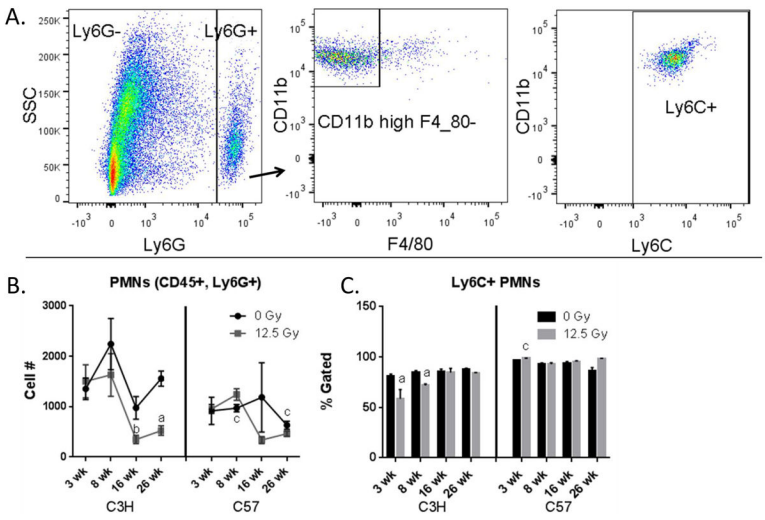

Figure 6.

Characterization of granulocytes. Lung cells from C3H and C57 mice, collected 3–26 wk following exposure of to 0 Gy or 12.5 Gy whole lung irradiation, were analyzed by flow cytometry. 6A: granulocytes were identified by first gating on the CD45+, Ly6G+ population and were analyzed for their expression of Ly6C, CD11b and F4/80. One representative sample is shown. 6B: Radiation-induced alterations in granulocyte cell number. 6C: Radiation-induced alterations in the proportion of Ly6C+ granulocytes. Each bar represents mean ± SEM (n = 3–4 mice/treatment group). [a]Significantly different from age-matched controls. [b]Significantly different from 3 wk time point (controls only). [c]Significantly different from C3H mice.